ARTICLE

Check for updates

Anorexia nervosa is associated with higher brain mu-opioid receptor availability

Kyoungjune Pak [1,2 ✉], Jouni Tuisku[3,4], Henry K. Karlsson [3,4,5,6], Jussi Hirvonen[3,4,7], Eleni Rebelos[3,4,8], Laura Pekkarinen [3,4,9], Lihua Sun [3,4,10], Aino Latva-Rasku [3,4], Semi Helin[3], Johan Rajander[11], Max Karukivi [3,4,5], Pirjo Nuutila [3,4,9] and Lauri Nummenmaa [3,4,12]

Anorexia nervosa (AN) is a severe psychiatric disorder, characterized by restricted eating, fear to gain weight, and a distorted body image. Mu-opioid receptor (MOR) functions as a part of complex opioid system and supports both homeostatic and hedonic control of eating behavior. Thirteen patients with AN and thirteen healthy controls (HC) were included in this study. We measured (1) MOR availability with [^{11}C]carfentanil positron emission tomography (PET), (2) brain glucose uptake (BGU) with 2-deoxy-2[^{18}F]fluoro-D-glucose ([^{18}F]FDG) PET during hyperinsulinemic-euglycemic clamp and (3) blood-oxygen-level-dependent signal with functional magnetic resonance imaging. All subjects underwent a screening visit consisting of physical examination, anthropometric measurements, fasting blood samples, an oral glucose tolerance test, psychiatric assessment, and an inquiry regarding medical history. Body fat mass (%) was measured and M value was calculated. MOR availability from caudate and putamen was higher in patients with AN and those from nucleus accumbens (NAcc) and thalamus showed the higher trend in patients with AN. There was no area where MOR availability was lower in patients with AN. BGU was not different between AN and HC. MOR availability and BGU were negatively correlated in caudate, NAcc and thalamus and showed the trend of negative association in putamen. In conclusion, AN is associated with higher MOR availability in the brain regions implicated in reward processing, while BGU remains unaltered. Therefore, the endogenous opioid system might be one of the key components underlying AN. This better understanding of AN could support the development of new treatments for AN.

Molecular Psychiatry; https://doi.org/10.1038/s41380-025-02888-3

INTRODUCTION

Anorexia nervosa (AN) is a severe psychiatric disorder, characterized by restricted eating, fear to gain the weight, and a distorted body image [1]. The peak age of AN onset is during adolescence, and more than 90% of AN patients are females [1]. The exact cause of AN is unknown, however, a combination of genetic, neurobiological, psychological and environmental factors might affect the development of AN [2]. Comorbidities of mood disorders, anxiety disorders, obsessive-compulsive disorders, autism spectrum disorder, and attention-deficit hyperactivity disorder are common in AN [3]. Also, patients with AN can have medical complications as a direct result of weight loss and malnutrition, such as hypoglycemia, osteoporosis, sarcopenia, cerebral atrophy, organ damage, and sudden death from arrhythmia [4].

Treatment of AN aims to restore body weight, mend the body image, eliminate the problematic eating patterns and develop long-term behavioral changes [3]. Current therapeutic approaches

of AN include psychotherapy, medications as well as dietary advice [3]. The prognosis of patients with AN remains however poor, with the highest mortality rate among all psychiatric disorders [1]. Among the surviving patients, less than 50% recover, whereas one third improve, and 20% remain chronically ill [5]. Therefore, understanding the pathophysiology of AN is crucial in the development of an effective treatment for AN.

Alterations of multiple neurotransmitter systems are linked with AN. Positron emission tomography (PET) using receptor or transporter binding radiopharmaceuticals has been utilized to understand the role of neurotransmitter systems in AN. Increased serotonin 1 A receptor of temporal, frontal lobes and amygdala [6], decreased serotonin 2 A receptor of frontal, parietal and occipital lobes [7] and increased cannabinoid 1 receptor of both cortical and subcortical areas [8] was reported with a regard to reward processing in eating behavior. However, there was no significant difference of dopamine receptor between patients with AN and healthy controls (HC) [9], although mesolimbic pathway in AN works

2

differently during reward learning and responding [10]. Also, fasting brain glucose uptake (BGU) was investigated with 2-deoxy-2[^{18}F] fluoro-D-glucose ([^{18}F]FDG) PET showing the inconsistent results of either global hypometabolism [11] or hypermetabolism of frontal lobe, hippocampus, amygdala and insula in AN [12].

The opioid system modulates motivation and reward processing and consequently is intimately linked with appetite and weight regulation [13]. Opioid agonists increase and opioid receptor antagonists decrease food intake and opioid receptor agonists stimulate food intake and the hedonic responses to palatable foods [14]. Feeding also leads to the release of endogenous opioid in humans [15]. In morbid obesity, mu-opioid receptor (MOR) availability was decreased [13] and weight loss after bariatric surgery normalizes MOR availability, suggesting weight-dependent regulation of MORs [16]. Also, lower MOR availability is associated with the increased familial obesity risk such as parental obesity or diabetes [17]. Therefore, MOR functions as a part of complex opioid system and supports both homeostatic and hedonic control of eating behavior [18].

Here, we investigated whether MOR and BGU are altered in patients with AN with comparison to HC. We used PET scans with MOR-specific ligand [^{11}C]carfentanil to quantify MOR availability and with [^{18}F]FDG during hyperinsulinemic, euglycemic clamp, to study brain glucose metabolism. Because AN is associated with fear of gaining weight when feeding, we also used anticipatory food reward protocol in fMRI to test whether acute affective responses to merely seeing food are altered consequences of the pathology [19]. We hypothesized that AN would be associated with the alteration of MOR with a regard to reward processing and BGU with a regard to insulin sensitivity.

MATERIALS AND METHODS
The study was conducted in accordance with the Declaration of Helsinki and approved by the Ethics Committee of the Hospital District of Southwest Finland. This study is a part of AVAIN project registered at ClinicalTrials.gov (Anorexia Nervosa and Its Effects on Brain Function, Body Metabolism and Their Interaction, NCT05101538). All participants signed ethics committee-approved informed consent forms prior to inclusion.

Subjects and study design
We recruited 13 patients with AN for the study. All patients with AN were required to meet the following criteria: (1) female, (2) age 18–32 years, (3) body mass index (BMI) < 17.5 kg/m^2, (4) currently fulfilling modified DSM-IV diagnosis of AN with or without amenorrhea, (5) AN onset before the age of 25 years, (6) no lifetime history of binge eating and (7) diagnosed less than 2 years ago. Patients with AN were compared with 13 HC who met the following criteria: (1) female, (2) age 18–32 years, (3) BMI 20–25 kg/m^2 and (4) no lifetime history of obesity (BMI ≥ 30 kg/m^2) or eating disorders. Exclusion criteria were any chronic disease or medication that would affect glucose metabolism or neurotransmission, history of psychiatric disorders (apart from AN), and abusive use of alcohol. Subjects underwent a screening consisting of physical examination, anthropometric measurements, fasting blood samples, a 75 g oral glucose tolerance test (OGTT), psychiatric assessment, and an inquiry regarding medical history. Body fat mass (%) was measured with an air displacement plethysmograph (the Bod Pod system, software version 5.4.0, COSMED, Inc., Concord, CA, USA) after at least 4 h of fasting. M value was calculated as a measure of insulin sensitivity as previously described [20] and expressed as per kilogram of fat-free mass, because this normalization minimizes differences due to sex, age, and body weight [21].

Brain PET acquisition
We measured MOR availability with high-affinity agonist radioligand [^{11}C] carfentanil with high sensitivity, and specificity for MORs. BGU was quantified with radioligand [^{18}F]FDG during hyperinsulinemic-euglycemic clamp. Scans were done on two separate visits. The subjects were advised to abstain from physical exercise in the PET scan days and the day before. PET studies were done after a 12-h overnight fast. Computed tomography scans were acquired before PET scans for attenuation correction. For [^{11}C]

carfentanil PET scan, a catheter was placed in the subject's left antecubital vein for tracer administration. After injection of [^{11}C]carfentanil, PET scan was acquired for 51 min using 13 frames of increasing duration (3*1 min, 4*3 min, 6*6 min). For [^{18}F]FDG PET scan, hyperinsulinemic-euglycemic clamp was applied as previously described [22, 23] to measure whole-body insulin sensitivity. After reaching steady glycemia, [^{18}F]FDG was injected intravenously and a peripheral scan for heart (5 min) and abdomen (25 min) was done before brain dynamic PET scan for 15 min (3 frames*5 min). Arterialized venous blood samples were taken to measure plasma activity, glucose, and insulin. The plasma radioactivity was measured by automatic gamma-counter (Wizard 1480 3″, Wallac, Turku, Finland). Anatomical T1-weighted magnetic resonance (MR) images (TR, 8.1 ms; TE, 3.7 ms; flip angle, 7°; scan time, 263 s; 1 mm^3 isotropic voxels) were obtained for anatomical normalization and reference; T2-weighted and fluid-attenuated inversion recovery (FLAIR) images were obtained to exclude significant brain pathology.

Brain PET analysis
PET images were preprocessed using an in-house automated processing tool (Magia [24]; https://github.com/tkkarjal/magia) running on MATLAB. Magia combines methods from SPM12 and FreeSurfer, two freely available and widely used tools with in-house software developed for kinetic modeling. Image processing began with motion-correction of the PET data followed by coregistration of the PET and MRI images. Magia aligns the frames, coregisters the PET image to each MRI, produces a reference region, calculates parametric images. Magia uses FreeSurfer (http://surfer.nmr.mgh.harvard.edu/) to define the regions of interest (ROIs) as well as the reference regions. The regional (ROI-wise) kinetic modeling was based on extracting ROI-wise time-activity curves. Voxel-wise parametric images were also generated, spatially normalized to MNI-space and finally smoothed using a Gaussian kernel. BGU-estimates (μmol/min/100 g) obtained from FDG PET data are based on fractional uptake rate multiplied by the average plasma glucose concentration from the injection until the end of the brain scan, divided by the lumped constant for the brain (set at 0.65) [25]. MOR availability was quantified by binding potential (BP_{ND}), which is the ratio of specific binding to non-displaceable binding in the tissue with simplified reference tissue model. Occipital cortex was used as the reference region [26].

fMRI acquisition
fMRI scans were acquired after overnight fasting. We used a previously established task protocol [19] for inducing anticipatory reward, by showing the participants pictures of palatable (for example, chocolate, pizza, cakes) and bland (for example, lentils, cereal, eggs) food pictures. This task simulates situations where appetite is triggered by anticipating the actual feeding via visual food cues, such as those in advertisements. The pictures were rated in a previous study by independent participants; the ratings showed that the appetizing foods were evaluated more pleasant than the bland foods, t(31) = 4.67, p < 0.001 [27]. During the tasks, functional data were acquired with gradient echo-planar imaging (EPI) sequence, sensitive to the blood-oxygen level-dependent imaging (BOLD) signal. Participants viewed alternating 16.2-s epochs with pictures of palatable or non-palatable foods. Each epoch contained nine stimuli from one category intermixed with fixation crosses. Each food stimulus was presented on either the right or the left side of the screen, and participants were instructed to indicate its location by pressing corresponding buttons. This task was used simply to ensure that participants had to pay attention to the stimuli. Stimulus delivery was controlled by the Presentation software (Neurobehavioral System, Inc.). Functional data were acquired using 3-Tesla Philips Ingenuity PET/MR scanner and using EPI sequence with the following parameters: TR, 2,600 ms; TE, 30 ms; flip angle 75°, 240*240*135 mm^3 FOV, 3*3*3 mm^3 voxel size. Each volume consisted of 45 interleaved axial slices acquired in ascending order. A total of 165 functional volumes were acquired, with additional five dummy volumes acquired and discarded at the beginning of each run. Anatomical reference images were acquired using a T1-weighted sequence with following parameters: TR 8.1 ms, TE 3.7 ms, flip angle 7°, 256*56*176 mm^3 FOV, 1*1*1 mm^3 voxel size.

fMRI analysis
Preprocessing of MRI images was performed using FMRIPREP (v.1.3.0.2) [28], a Nipype (v.1.1.9) [29] based tool. Each T1-weighted image was corrected for intensity non-uniformity with N4BiasFieldCorrection (v.2.1.0)

Table 1. Subjects' characteristics.

	Anorexia nervosa (n = 13)		Healthy controls (n = 13)		p
	Mean	Standard deviation	Mean	Standard deviation	
Age (years)	20.5	1.7	23.8	3.3	0.0044
Height (cm)	168.4	6.4	166.3	3.8	0.3175
Weight (kg)	47.5	4.9	63.1	5.0	<0.0001
Body mass index (kg/m^2)	16.7	1.2	22.8	1.9	<0.0001
Body fat mass (%)	20.2	7.5	33.6	5.4	<0.0001
Systolic blood pressure (mmHg)	102.6	6.9	113.5	10.7	0.0066
Diastolic blood pressure (mmHg)	64.8	4.7	76.8	9.1	0.0005
Blood glucose level (mmol/L)	5.0	0.3	5.1	0.3	0.4335
M value (µmol/(kg*min))	40.1	13.4	28.4	10.0	0.0197
Total cholesterol (mmol/L)	3.7	0.7	6.0	5.7	0.1830
Triglyceride (mmol/L)	0.6	0.3	1.3	1.2	0.0892
HDL cholesterol (mmol/L)	1.8	0.7	1.7	0.3	0.5612
LDL cholesterol (mmol/L)	3.1	3.7	2.5	0.4	0.5527
Injected activity of [^{11}C]carfentanil (MBq)	248.2	9.5	242.3	8.8	0.1175
Injected activity of [^{18}F]fluorodeoxyglucose (MBq)	150.6	7.0	150.2	6.5	0.8971

[30] and skull-stripped on the basis of the OASIS template with antsBrainExtraction. sh workflow (ANTs v.2.2.0). Brain surfaces were reconstructed using recon-all from FreeSurfer (v.6.0.0) [31], and the brain mask estimated previously was refined with a custom variation of the method to reconcile ANTs- and FreeSurfer-derived segmentations of the cortical gray matter using Mindboggle [32]. Spatial normalization to the ICBM 152 non-linear asymmetrical template v.2009c [33] was done with non-linear registration using the antsRegistration tool [34]. Tissue segmentation of cerebrospinal fluid, white matter and gray matter was performed on the brain-extracted T1w using fast [35] from FSL (v.5.0.9). fMRI images were slice time corrected with 3dTshift from AFNI (v.16.2.07) [36] and motion corrected with mcflirt [37] from FSL. This was followed by coregistration to the corresponding T1w via boundary-based registration [38] with nine degrees of freedom, using bbregister from FreeSurfer. These steps were concatenated and applied in a single step via antsApplyTransforms with the Lanczos interpolation. Physiological noise regressors were obtained using CompCor [39], where principal components were estimated for temporal and anatomical variants. A mask to exclude signal with cortical origin was created via eroding the brain mask, ensuring it merely originating from subcortical structures. Six temporal CompCor components were then calculated including the top 5% variable voxels within that subcortical mask. For anatomical CompCor components, six components were calculated within the intersection of the subcortical mask and the union of cerebral spinal fluid and white matter masks, after projection to the native space of each functional run. Frame-wise displacement [40] was calculated for each functional run using the implementation of Nipype. Finally, ICA-based automatic removal of motion artifacts was used to generate aggressive noise regressors and also to create a variant of data that is non-aggressively denoised [41]. The quality of images was assessed using FMRIPREP's visual reports, where data were manually inspected for whole-brain field of view coverage, alignment to the anatomical images and artifacts. fMRI data were analyzed using SPM 12 with MATLAB (v.R2016b). Whole-brain random effects model was applied using a two-stage process with separate first and second levels. For each participant, the general linear model was first used to predict regional effects of task parameters (palatable and non-palatable foods). Participant-wise contrast images were generated for the effect of palatable versus non-palatable foods, and subjected to second-level analyses. The results were thresholded with false discovery rate with p < 0.05 using SPM 12.

Statistical analysis
Data are presented as mean ± standard deviation. Normality of data distribution was tested with Shapiro-Wilk test. Two-sample t-test was used to compare MOR availability and BGU between groups. The results were corrected using the Bonferroni method ROIs (p < 0.05/11 = 0.0045). Two-sample t-test was used to compare subjects' characteristics across groups. Pearson correlation analysis was used to determine the association

between MOR availability, BGU and BMI, M value. Statistical analysis was carried out in R Statistical Software (The R Foundation for Statistical Computing). For a full-volume comparison between patients with AN and HC, the statistical threshold in statistical parametric mapping analysis was set at a cluster level and corrected with false discovery rate with p < 0.05 using SPM 12.

RESULTS
Subject characteristics
Thirteen patients with AN (20.5 ± 1.7 years) and thirteen HC (23.8 ± 3.3 years) were enrolled in this study. The key characteristics of the study groups are shown in Table 1. As expected, patients in the AN group had significantly lower BMI (16.7 ± 1.2 kg/m^2 vs 22.8 ± 1.9 kg/m^2; p < 0.0001), body fat mass (20.2 ± 7.5% vs 33.6 ± 5.4%; p < 0.0001), systolic blood pressure (102.6 ± 6.9 mmHg vs 113.5 ± 10.7 mmHg; p = 0.0066) and diastolic blood pressure (64.8 ± 4.7 mmHg vs 76.8 ± 9.1 mmHg; p = 0.0005) as compared to HC. Whole body insulin sensitivity M-value measured with hyperinsulinemic-euglycemic clamp per body weight and minute was significantly higher in AN than HC (40.1 ± 13.4 µmol/(kg*min) vs 28.4 ± 10.0 µmol/(kg*min); p = 0.0197). All subjects underwent both [^{11}C]carfentanil and [^{18}F]FDG brain PET scans except for one patient with AN who did not participate in the [^{18}F]FDG PET scan.

MOR availability, BGU, and BOLD signal
MOR availability in the caudate (p = 0.0192) and putamen (p = 0.0264) was higher in AN than in HC, and those in nucleus accumbens (NAcc) (p = 0.0504) and thalamus (p = 0.0850) showed the higher trend in patients with AN before correction for multiple comparison, these results however did not survive after correction for multiple comparison (Fig. 1). Averaged images of [^{11}C]carfentanil PET in patients with AN and HC are presented in Fig. 2. In full-volume analysis, higher MOR availability was observed from caudate, putamen, NAcc, thalamus, and orbitofrontal cortex in patients with AN (Fig. 3). However, in [^{18}F]FDG PET scans, BGU was not significantly different between patients with AN and HC in both ROI analysis and voxel-wise analysis. MOR availability and BGU were negatively correlated in caudate (r = −0.4680; p = 0.0183), NAcc (r = −0.4310; p = 0.0315) and thalamus (r = −0.4094; p = 0.0421) and showed the trend of negative association in putamen (r = −0.3880; p = 0.0553) (Fig. 4). In a subgroup analysis, MOR availability and BGU were negatively correlated in caudate
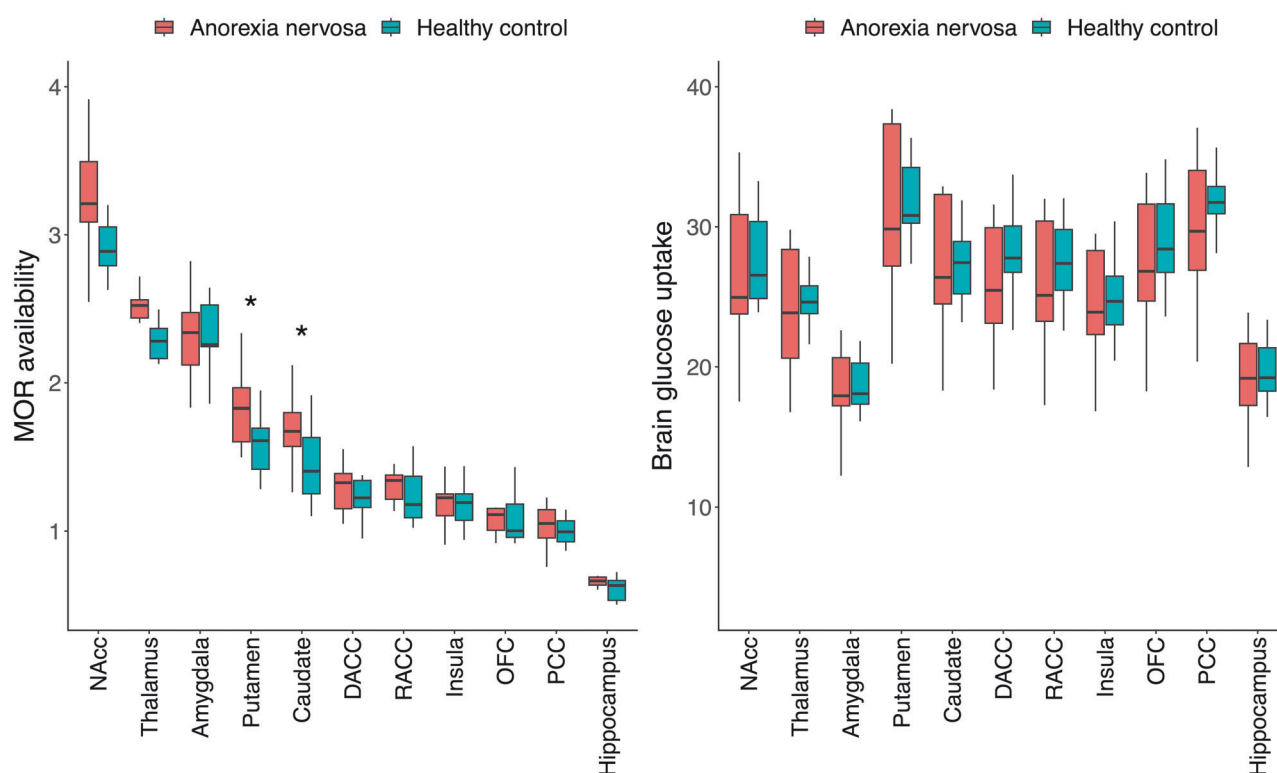
Fig. 1 Comparison between patients with AN and HC. Left MOR availability in the caudate and putamen was higher in patients with AN than in HC, Right BGU was not significantly different between patients with AN and HC.
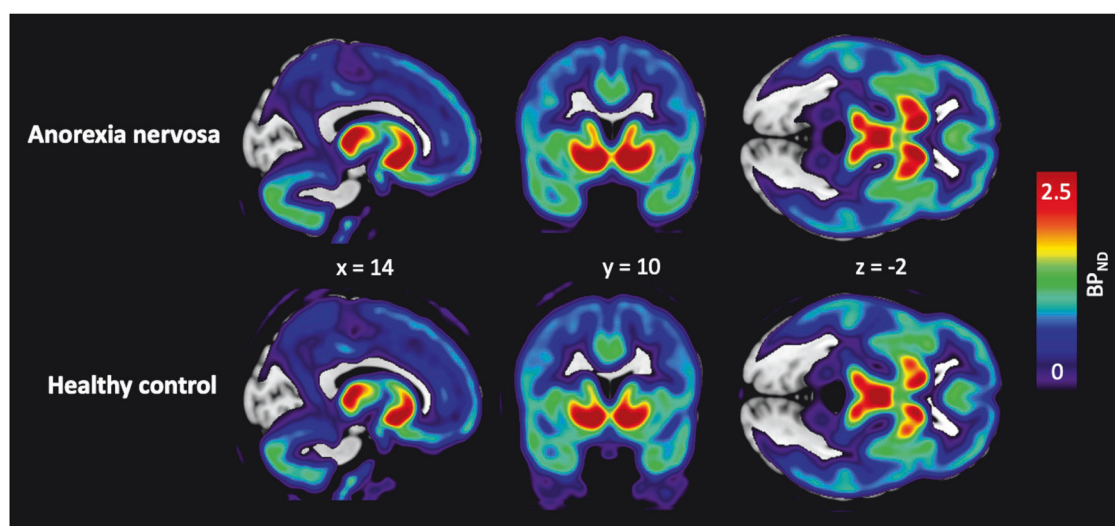

Fig. 2 Averaged images of [^{11}C]carfentanil PET. Upper patients with AN, Lower HC.

(r = −0.6153; p = 0.0332), NAcc (r = −0.6801; p = 0.0149) and thalamus (r = −0.6173; p = 0.0325) of patients with AN, not in those of HC (Supplementary fig. 1). In addition, there was no difference of hemodynamic brain activity of viewing palatable versus non-palatable foods between patients with AN and HC.

DISCUSSION

Our main finding is that MOR availability in patients with AN was higher in brain regions implicated in reward processing, while BGU was not different between patients with AN and HC. Negative correlation between MOR availability and BGU was observed in

caudate, NAcc, and thalamus. The effect of upregulated MOR availability is a mirror image of the downregulated MOR system in obesity [13, 16, 42]. Studies have also found that upregulation of MORs occurs following weight loss [16, 42]. Altogether these data show how cerebral glucose metabolism is maintained in typical levels even under severe undernutrition, whereas central MOR systems adapt to the peripheral dysregulation, potentially contributing to the mood changes in patients with AN.

Upregulated Mu-opioid receptor availability in AN

AN is a severe psychiatric disorder characterized by an extremely low body weight, fear to gain weight and a distorted body image
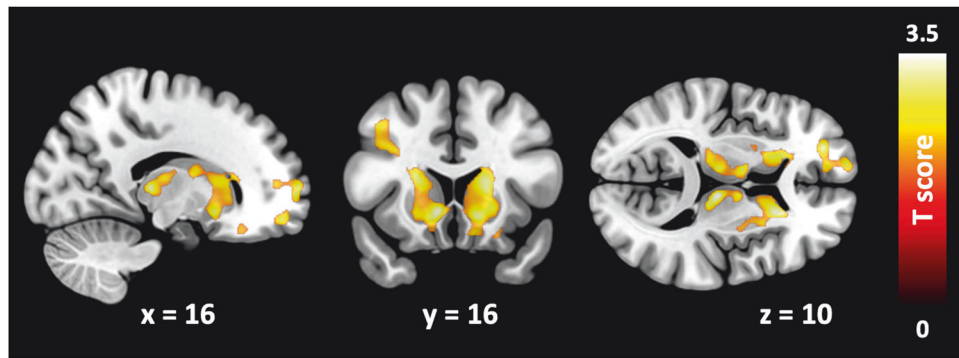
Fig. 3 Comparison of [^{11}C]carfentanil PET scans between patients with AN and HC. Higher MOR availability was observed from caudate, putamen, NAcc, thalamus, and orbitofrontal cortex in patients with AN.
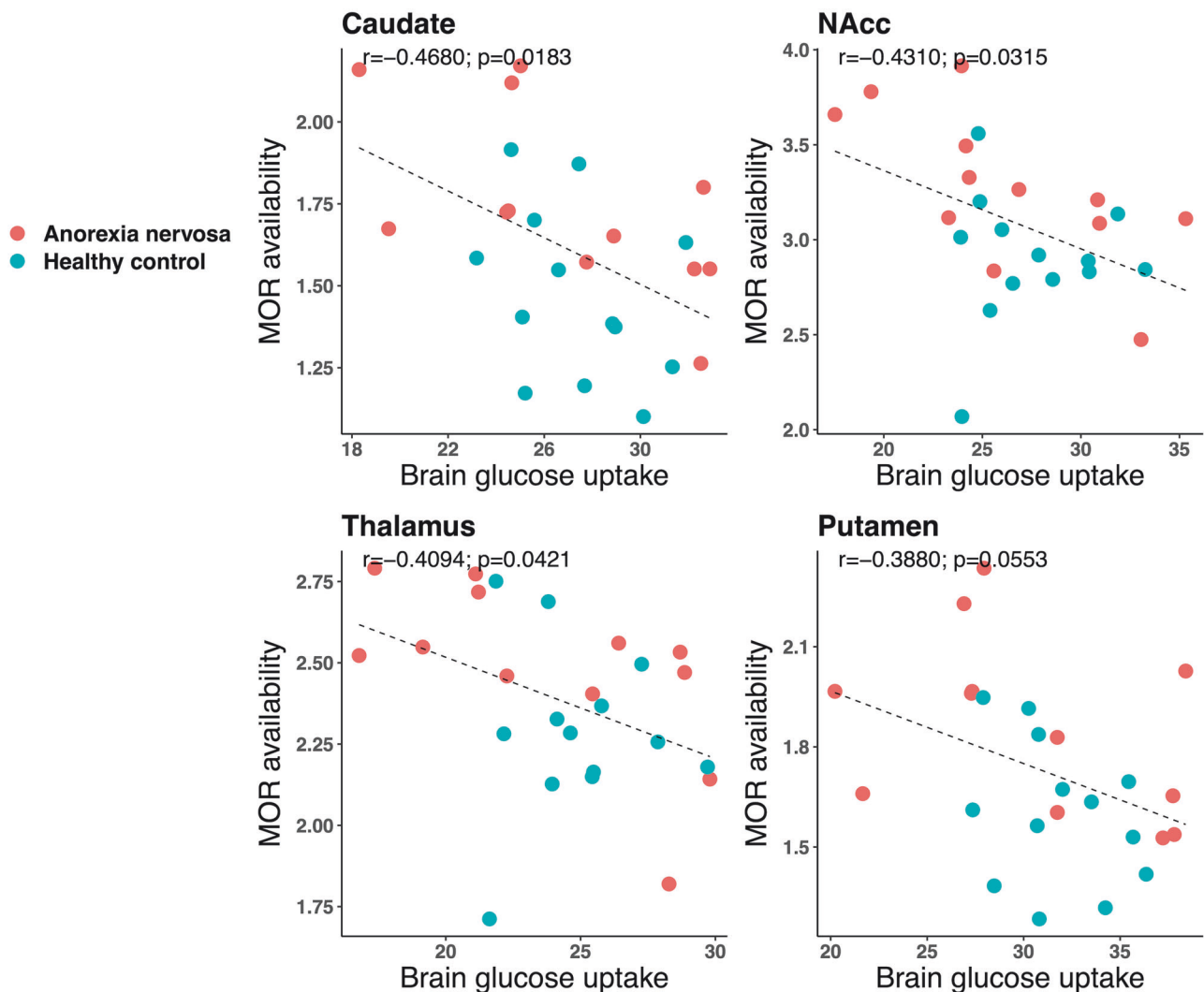

Fig. 4 Correlations between MOR availability (BP$_{ND}$) and BGU (µmol/min/100 g). MOR availability and BGU were negatively correlated in caudate, NAcc and thalamus and showed the trend of negative association in putamen.

with comorbid mood disorders, major depressive disorders, anxiety disorders, obsessive-compulsive disorders, autism and attention-deficit hyperactivity disorder [3]. The etiology of AN is complicated and involves genetic, neurobiological, psychological and environmental factors [2]. Some patients with AN start losing the weight voluntarily and after several months, they have a positive experience with losing the weight, however, facing a difficulty to

eat normally, causing discomfort and anxiety [2]. As they have amplified negative experiences when trying to eat normally, the vicious cycle of AN is established [2]. The treatment of AN includes medical care such as monitoring of vital signs and hydration, diet and psychotherapy to restore a healthy weight [2]. However, the prognosis of AN is still poor with the highest mortality rate among all psychiatric disorders [1]. In addition, post-treatment relapse rates

exceed 30% [43]. Thus, central molecular pathways contributing to feeding, mood, and reward would be linked with AN.

In line with this hypothesis, we found that central MOR upregulation was observed in patients with AN. The endogenous opioid system and particularly MORs are associated with both homeostatic and hedonic control of eating behavior [18] as well as mood regulation [44]. Opioid antagonists decrease food intake and opioid receptor agonists stimulate food intake and the hedonic responses to palatable foods [14]. Consumption of both palatable and nonpalatable meals triggers release of endogenous opioids [15] and this response is more pronounced following a nonpalatable versus palatable meal. Therefore, opioid release can be modulated by individuals' current metabolic state. To control for this, our participants underwent 12-h overnight fasting, prior to PET scans, minimizing the potential effect of acute nutritional status. However, factors related to long-term feeding preferences cannot be ruled out in the current design. Individual variation in MOR is also associated with anticipatory reward responses, and lowered MOR availability is linked with stronger BOLD fMRI responses to appetizing foods in frontal and cingulate cortices, striatum and amygdala of the reward and emotion circuit [19]. In the present study, upregulated MOR availability in patients with AN was observed in brain regions implicated in reward processing, which might be associated with reduced pleasure in eating behavior, a refusal to eat and this would lead to a vicious cycle of AN. This result is also in line with previous studies in obesity. Our group has previously shown that MOR availability is higher in nonobese subjects than morbidly obese subjects (22.7 ± 2.9 kg/m^2 vs 41.9 ± 3.9 kg/m^2) [13], and that was higher in patients with AN than HC (16.7 ± 1.2 kg/m^2 vs 22.8 ± 1.9 kg/m^2) in this study. Thus, it is possible that the MOR availability scales with BMI with highest availability in patients with AN and lowest in morbidly obese subjects, with HC in between. However, explanations based on reward-based versus metabolically driven alterations are not mutually exclusive, and cannot be dissociated in the present cross-sectional study.

Prior studies have found no difference of striatal dopamine receptor availability between patients with AN and HC [9], however, there is a possibility of MOR-induced disruption of the reward pathway through dopamine system in AN, which was reported in morbid obesity [45]. One previous study with [^{11}C]diprenorphine, a non-selective opioid receptor radiopharmaceutical, compared opioid receptor availability between patients with AN and HC [46]. Interestingly, opioid receptor availability was lower (rather than higher as in our study) in anterior cingulate cortex, insula, frontal, temporal and parietal lobes, suggesting the potential involvement of reward circuit modulation and anxiety in AN [46].

In addition to MORs, other neurotransmitter systems have been linked with AN. Increased serotonin 1 A receptor of temporal, frontal lobes and amygdala [6] and decreased serotonin 2 A receptor of frontal, parietal and occipital lobes [7] in patients with AN versus HC have been reported. Also, cannabinoid 1 receptor availability is increased in both cortical and subcortical areas in patients with AN [8]. Involvement of serotonin and cannabinoid systems in AN is not surprising as both have an important role in eating behavior regarding reward pathway. Finally, histamine 1 receptor of limbic system, particularly amygdala was significantly higher in AN with a possibility of the involvement of histamine system in psychological symptoms such as emotional changes to food and body image as well as eating behavior [47]. However, no significant difference of dopamine receptor between patients with AN and HC [9] has been reported, although mesolimbic pathway in AN works differently during reward learning and responding [10].

Brain glucose uptake
In addition to MOR availability, we contrasted BGU between patients with AN and HC. Although there was no difference in BGU between patients with AN and HC, a negative correlation of M value, a measure of insulin sensitivity, with BGU was observed, consistent with previous findings [48]. Global cerebral

hypometabolism was observed in patients with AN using dynamic acquisition of [^{18}F]FDG PET without hyperinsulinemic-euglycemic clamp [11]. This altered brain glucose metabolism may be a consequence of low body weight and prolonged starvation state induced acido-ketosis [49] or a morphologic factor such as enlargement of cortical sulci and ventricles [50] or changes in the permeability of blood vessels [11]. However, another study with static acquisition of [^{18}F]FDG PET, hypermetabolism of frontal lobe, hippocampus, amygdala, insula and hypometabolism of parietal lobe was reported [12]. The method of [^{18}F]FDG PET acquisition might affect the result of BGU in AN and HC and, currently, [^{18}F]FDG PET during hyperinsulinemic euglycemic clamp is the gold standard for measuring regional tissue glucose uptake rates [51]. A negative correlation between MOR availability and BGU was observed in the same brain regions that showed the higher MOR availability in AN. These data show that BGU is maintained despite the overall poor metabolic states of patients with AN, could indicate that the brains have to be kept up and running at all costs. In addition, there is a possibility of altered MOR leading to the constant BGU state by the interaction between MOR and BGU in patients with AN.

BOLD signal
No differences were found in the acute food-related affective between patients with AN and HC, possibly due to small sample sizes and challenges in the recruitment of participants. We used appetitive and bland food images to assess food reward responses, as in our previous studies [19, 52], but did not gather in situ data on participants' food preferences. Differences in taste preferences between patients with AN and HC may have confounded the results.

Strengths and limitations
Our study has provided deep phenotypical evaluation of patients with AN and matched HC. The combination for the first time of two PET tracers is also a considerable strength. Our study also has limitations. First, as AN is more predominant in females, we included only females with AN in this study. Therefore, the results may not be applicable in males. Second, as patients with AN may be particularly sensitive to questions regarding their eating behavior, we did not perform a questionnaire of eating behavior on participants so we could not link the changes in MOR availability and BGU with their eating behaviors. Third, the study was relatively small with 13 subjects in each group. The sample size was limited by the complex multimodal imaging setup, however, significant effects were nonetheless observed. Fourth, higher MOR availability from [^{11}C]carfentanil PET BP$_{ND}$ may reflect either an increased number of receptor proteins or an increased affinity to bind this radioligand agonists and it remains unclear whether this change in opioid system is the cause or the result of AN. Finally, small brain structures such as NAcc may be affected by partial volume effects. Therefore, we analyzed PET scans both with and without partial volume correction (PVC) and found that the results were consistent with both approaches. Brain regions showing higher MOR availability in patients with AN versus HC (FDR corrected $p < 0.05$) with PVC are shown in Supplementary figure 2.

AN is associated with higher MOR availability in the brain regions implicated in reward processing, while BGU remains unaltered. Therefore, the endogenous opioid system might be one of the key components underlying AN and concomitant alterations in food intake and mood. The better understanding of the pathophysiology of AN could eventually lead to the development of new treatments for AN.

DATA AVAILABILITY
The data that support the findings of this study are available from the corresponding author upon reasonable request.

REFERENCES

1. Kaye WH, Fudge JL, Paulus M. New insights into symptoms and neurocircuit function of anorexia nervosa. Nat Rev Neurosci. 2009;10:573–84.
2. Frostad S, Bentz M. Anorexia nervosa: outpatient treatment and medical management. World J Psychiatry. 2022;12:558–79.
3. Watson HJ, Yilmaz Z, Thornton LM, Hubel C, Coleman JRI, Gaspar HA, et al. Genome-wide association study identifies eight risk loci and implicates metabo-psychiatric origins for anorexia nervosa. Nat Genet. 2019;51:1207–14.
4. Mehler PS, Brown C. Anorexia nervosa - medical complications. J Eat Disord. 2015;3:11.
5. Steinhausen HC. The outcome of anorexia nervosa in the 20th century. Am J Psychiatry. 2002;159:1284–93.
6. Galusca B, Costes N, Zito NG, Peyron R, Bossu C, Lang F, et al. Organic background of restrictive-type anorexia nervosa suggested by increased serotonin 1A receptor binding in right frontotemporal cortex of both lean and recovered patients: [18F]MPPF PET scan study. Biol Psychiatry. 2008;64:1009–13.
7. Audenaert K, Van Laere K, Dumont F, Vervaet M, Goethals I, Slegers G, et al. Decreased 5-HT2a receptor binding in patients with anorexia nervosa. J Nucl Med. 2003;44:163–9.
8. Gerard N, Pieters G, Goffin K, Bormans G, Van Laere K. Brain type 1 cannabinoid receptor availability in patients with anorexia and bulimia nervosa. Biol Psychiatry. 2011;70:777–84.
9. Broft A, Slifstein M, Osborne J, Kothari P, Morim S, Shingleton R, et al. Striatal dopamine type 2 receptor availability in anorexia nervosa. Psychiatry Res. 2015;233:380–7.
10. Frank GK, Reynolds JR, Shott ME, Jappe L, Yang TT, Tregellas JR, et al. Anorexia nervosa and obesity are associated with opposite brain reward response. Neuropsychopharmacology. 2012;37:2031–46.
11. Delvenne V, Lotstra F, Goldman S, Biver F, De Maertelaer V, Appelboom-Fondu V, et al. Brain hypometabolism of glucose in anorexia nervosa: a PET scan study. Biol Psychiatry. 1995;37:161–9.
12. Zhang HW, Li DY, Zhao J, Guan YH, Sun BM, Zuo CT. Metabolic imaging of deep brain stimulation in anorexia nervosa: a 18F-FDG PET/CT study. Clin Nucl Med. 2013;38:943–8.
13. Karlsson HK, Tuominen L, Tuulari JJ, Hirvonen J, Parkkola R, Helin S, et al. Obesity is associated with decreased mu-opioid but unaltered dopamine D2 receptor availability in the brain. J Neurosci. 2015;35:3959–65.
14. Pecina S, Berridge KC. Hedonic hot spot in nucleus accumbens shell: where do mu-opioids cause increased hedonic impact of sweetness? J Neurosci. 2005;25:11777–86.
15. Tuulari JJ, Tuominen L, de Boer FE, Hirvonen J, Helin S, Nuutila P, et al. Feeding releases endogenous opioids in humans. J Neurosci. 2017;37:8284–91.
16. Karlsson HK, Tuulari JJ, Tuominen L, Hirvonen J, Honka H, Parkkola R, et al. Weight loss after bariatric surgery normalizes brain opioid receptors in morbid obesity. Mol Psychiatry. 2016;21:1057–62.
17. Kantonen T, Pekkarinen L, Karjalainen T, Bucci M, Kalliokoski K, Haaparanta-Solin M, et al. Obesity risk is associated with altered cerebral glucose metabolism and decreased mu-opioid and CB(1) receptor availability. Int J Obes. 2022;46:400–7.
18. Valbrun LP, Zvonarev V. The opioid system and food intake: use of opiate antagonists in treatment of binge eating disorder and abnormal eating behavior. J Clin Med Res. 2020;12:41–63.
19. Nummenmaa L, Saanijoki T, Tuominen L, Hirvonen J, Tuulari JJ, Nuutila P, et al. mu-opioid receptor system mediates reward processing in humans. Nat Commun. 2018;9:1500.
20. Iozzo P, Gastaldelli A, Jarvisalo MJ, Kiss J, Borra R, Buzzigoli E, et al. 18F-FDG assessment of glucose disposal and production rates during fasting and insulin stimulation: a validation study. J Nucl Med. 2006;47:1016–22.
21. Gastaldelli A, Casolaro A, Pettiti M, Nannipieri M, Ciociaro D, Frascerra S, et al. Effect of pioglitazone on the metabolic and hormonal response to a mixed meal in type II diabetes. Clin Pharmacol Ther. 2007;81:205–12.
22. DeFronzo RA, Tobin JD, Andres R. Glucose clamp technique: a method for quantifying insulin secretion and resistance. Am J Physiol. 1979;237:E214–223.
23. Nuutila P, Koivisto VA, Knuuti J, Ruotsalainen U, Teras M, Haaparanta M, et al. Glucose-free fatty acid cycle operates in human heart and skeletal muscle in vivo. J Clin Invest. 1992;89:1767–74.
24. Karjalainen T, Tuisku J, Santavirta S, Kantonen T, Bucci M, Tuominen L, et al. Magia: robust automated image processing and kinetic modeling toolbox for PET neuroinformatics. Front Neuroinform. 2020;14:3.
25. Thie JA. Clarification of a fractional uptake concept. J Nucl Med. 1995;36:711–2.
26. Frost JJ, Douglass KH, Mayberg HS, Dannals RF, Links JM, Wilson AA, et al. Multicompartmental analysis of [11C]-carfentanil binding to opiate receptors in humans measured by positron emission tomography. J Cereb Blood Flow Metab. 1989;9:398–409.
27. Nummenmaa L, Hirvonen J, Hannukainen JC, Immonen H, Lindroos MM, Salminen P, et al. Dorsal striatum and its limbic connectivity mediate abnormal anticipatory reward processing in obesity. PLoS One. 2012;7:e31089.
28. Esteban O, Markiewicz CJ, Blair RW, Moodie CA, Isik AI, Erramuzpe A, et al. fMRIPrep: a robust preprocessing pipeline for functional MRI. Nat Methods. 2019;16:111–6.
29. Gorgolewski K, Burns CD, Madison C, Clark D, Halchenko YO, Waskom ML, et al. Nipype: a flexible, lightweight and extensible neuroimaging data processing framework in python. Front Neuroinform. 2011;5:13.
30. Tustison NJ, Avants BB, Cook PA, Zheng Y, Egan A, Yushkevich PA, et al. N4ITK: improved N3 bias correction. IEEE Trans Med Imaging. 2010;29:1310–20.
31. Dale AM, Fischl B, Sereno MI. Cortical surface-based analysis. I. Segmentation and surface reconstruction. Neuroimage. 1999;9:179–94.
32. Klein A, Ghosh SS, Bao FS, Giard J, Hame Y, Stavsky E, et al. Mindboggling morphometry of human brains. PLoS Comput Biol. 2017;13:e1005350.
33. Fonov V, Evans AC, Botteron K, Almli CR, McKinstry RC, Collins DL, et al. Unbiased average age-appropriate atlases for pediatric studies. Neuroimage. 2011;54:313–27.
34. Avants BB, Epstein CL, Grossman M, Gee JC. Symmetric diffeomorphic image registration with cross-correlation: evaluating automated labeling of elderly and neurodegenerative brain. Med Image Anal. 2008;12:26–41.
35. Zhang Y, Brady M, Smith S. Segmentation of brain MR images through a hidden Markov random field model and the expectation-maximization algorithm. IEEE Trans Med Imaging. 2001;20:45–57.
36. Cox RW. AFNI: software for analysis and visualization of functional magnetic resonance neuroimages. Comput Biomed Res. 1996;29:162–73.
37. Jenkinson M, Bannister P, Brady M, Smith S. Improved optimization for the robust and accurate linear registration and motion correction of brain images. Neuroimage. 2002;17:825–41.
38. Greve DN, Fischl B. Accurate and robust brain image alignment using boundary-based registration. Neuroimage. 2009;48:63–72.
39. Behzadi Y, Restom K, Liau J, Liu TT. A component based noise correction method (CompCor) for BOLD and perfusion based fMRI. Neuroimage. 2007;37:90–101.
40. Power JD, Mitra A, Laumann TO, Snyder AZ, Schlaggar BL, Petersen SE. Methods to detect, characterize, and remove motion artifact in resting state fMRI. Neuroimage. 2014;84:320–41.
41. Pruim RHR, Mennes M, van Rooij D, Llera A, Buitelaar JK, Beckmann CF. ICA-AROMA: a robust ICA-based strategy for removing motion artifacts from fMRI data. Neuroimage. 2015;112:267–77.
42. Burghardt PR, Rothberg AE, Dykhuis KE, Burant CF, Zubieta JK. Endogenous opioid mechanisms are implicated in obesity and weight loss in humans. J Clin Endocrinol Metab. 2015;100:3193–201.
43. Berends T, Boonstra N, van Elburg A. Relapse in anorexia nervosa: a systematic review and meta-analysis. Curr Opin Psychiatry. 2018;31:445–55.
44. Nummenmaa L, Karjalainen T, Isojärvi J, Kantonen T, Tuisku J, Kaasinen V, et al. Lowered endogenous mu-opioid receptor availability in subclinical depression and anxiety. Neuropsychopharmacology. 2020;45:1953–9.
45. Tuominen L, Tuulari J, Karlsson H, Hirvonen J, Helin S, Salminen P, et al. Aberrant mesolimbic dopamine-opiate interaction in obesity. Neuroimage. 2015;122:80–6.
46. Galusca B, Traverse B, Costes N, Massoubre C, Le Bars D, Estour B, et al. Decreased cerebral opioid receptors availability related to hormonal and psychometric profile in restrictive-type anorexia nervosa. Psychoneuroendocrinology. 2020;118:104711.
47. Yoshizawa M, Tashiro M, Fukudo S, Yanai K, Utsumi A, Kano M, et al. Increased brain histamine H1 receptor binding in patients with anorexia nervosa. Biol Psychiatry. 2009;65:329–35.
48. Rebelos E, Bucci M, Karjalainen T, Oikonen V, Bertoldo A, Hannukainen JC, et al. Insulin resistance is associated with enhanced brain glucose uptake during euglycemic hyperinsulinemia: a large-scale PET cohort. Diabetes Care. 2021;44:788–94.
49. Herholz K, Krieg JC, Emrich HM, Pawlik G, Beil C, Pirke KM, et al. Regional cerebral glucose metabolism in anorexia nervosa measured by positron emission tomography. Biol Psychiatry. 1987;22:43–51.
50. Enzmann DR, Lane B. Cranial computed tomography findings in anorexia nervosa. J Comput Assist Tomogr. 1977;1:410–4.
51. Rebelos E, Mari A, Oikonen V, Iida H, Nuutila P, Ferrannini E. Evaluation of renal glucose uptake with [(18)F]FDG-PET: methodological advancements and metabolic outcomes. Metabolism. 2023;141:155382.
52. Laurila S, Sun L, Lahesmaa M, Schnabl K, Laitinen K, Klen R, et al. Secretin activates brown fat and induces satiation. Nat Metab. 2021;3:798–809.

AUTHOR CONTRIBUTIONS

COMPETING INTERESTS

ADDITIONAL INFORMATION